

A&A manuscript no.

(will be inserted by hand later)

Your thesaurus codes are:

03 (11.09.1 M 31; 11.09.4; 09.09.1 D 478 09.13.2, 13.19.1)

Detection of neutral carbon in the M 31 dark cloud D 478

F.P. Israel¹ and R.P.J. Tilanus^{2,3} and F. Baas^{1,2}

¹ Sterrewacht Leiden, P.O. Box 9513, NL 2300 RA Leiden, The Netherlands

² Joint Astronomy Centre, 660 N. A'ohoku Pl., Hilo, Hawaii, 96720, USA

³ Netherlands Foundation for Research in Astronomy, P.O. Box 2, NL 7990 AA Dwingeloo, The Netherlands

Received 17 April 1998; accepted 7 July 1998

Abstract. Emission from the $^3P_1 - ^3P_0$ [CI] transition at 492 GHz has been detected towards the dark cloud D 478 in the Local Group galaxy M 31. Using literature detections of the lower ^{12}CO and ^{13}CO transitions, models for the gas distribution in D 478 are discussed. The observed CO and C line ratios can be explained by two-component models (high density cores and low-density envelopes); single-density models appear less likely. The models indicate kinetic temperatures of the order of $T_k \approx 10$ K. The beam-averaged column density of neutral carbon is 0.3–0.8 times that of CO, whereas the total carbon to hydrogen ratio N_C/N_H is $5-3 \times 10^{-4}$. The resulting CO to H_2 conversion factor X is about half that of the Solar Neighbourhood. With temperatures of about 10 K and projected mass-densities of $5-10 M_\odot \text{ pc}^{-2}$ there appears to be no need to invoke the presence of very cold and very massive clouds. Rather, D 478 appears to be comparable to Milky Way dark cloud complexes at the higher metallicity expected from its central location in M 31. In particular, several similarities between D 478 and the Galactic Taurus-Auriga dark cloud complex may be noted.

Key words: Galaxies – individual (M 31) – ISM; ISM – individual (D 478) – molecules; Radio lines – galaxies

1. Introduction

Several molecular cloud complexes have been detected in the spiral arms of the Local Group galaxy M 31 by their $^{12}\text{CO } J=1-0$ emission (Blitz 1985; Ryden & Stark 1986; Vogel et al. 1987; Casoli et al. 1987; Nakano et al. 1987; Lada et al. 1988; Casoli & Combes 1988; Berkhuijsen et al. 1993; Wilson & Rudolph 1993; Loinard et al. 1996b). Most appear to be giant molecular cloud complexes similar to those in the disk of the Milky Way (Vogel et al 1987; Lada et al. 1988; Wilson & Rudolph 1993). However, Blitz (1985) noted velocity widths systematically higher than expected on the basis of the observed integrated line intensities. He proposed that the observed CO emission is

from both GMC's and small clouds, and dominated by the contribution from the latter. Maps of a northeastern spiral arm of M 31 by Casoli et al. (1987) and Casoli & Combes (1988) and a southwestern spiral arm by Kutner et al. (1990) provide evidence for a dual population: in addition to major complexes that have the characteristics of 'normal' GMC's, additional CO emission appears to originate from numerous small clouds. Unbiased CO surveys along the minor and major axes of M 31 have been carried out by Sandqvist et al. (1989) and Loinard et al. (1995) respectively. The former found relatively strong CO emission associated with M 31 spiral arm '4' and weaker CO emission from the outer warp. The latter found CO emission in the majority of positions sampled, in a number of cases without a counterpart dust cloud. They also found generally low $^{12}\text{CO } J=2-1/J=1-0$ ratios which they interpreted as arising from cold ($T_k < 5$ K) molecular clouds at low density ($n_{\text{H}_2} \approx 100 \text{ cm}^{-3}$).

In addition, they observed several dust clouds (Hodge 1980) in the inner parts of M 31 (Allen & Lequeux 1993; Loinard et al. 1996a). Two of these, D 268 and D 478 were observed in the lower two transitions of both ^{12}CO and ^{13}CO and subsequently modelled in detail by Allen et al. (1995). They conclude that the ^{12}CO emission is dominated by a very cold, low-density gas, while the ^{13}CO emission comes largely from higher-density clumps inside the clouds. In an attempt to further investigate the unusual physical conditions of these molecular clouds, we have observed the strongest of these two objects, D 478, in the neutral carbon line. While this work was in progress, an interferometric map of the $^{12}\text{CO } J=1-0$ distribution, and the $^{12}\text{CO } J=3-2$ profile of D 478 have also become available (Loinard & Allen 1998).

2. Observations

The observations were carried out with the 15m James Clerk Maxwell Telescope (JCMT) on Mauna Kea (Hawaii)¹. The $^3P_1 - ^3P_0$ [CI] transition at $\nu = 492.161$ GHz was observed towards D 478 for a total integration time of 100

¹ The James Clerk Maxwell Telescope is operated by The Joint Astronomy Centre on behalf of the Particle Physics

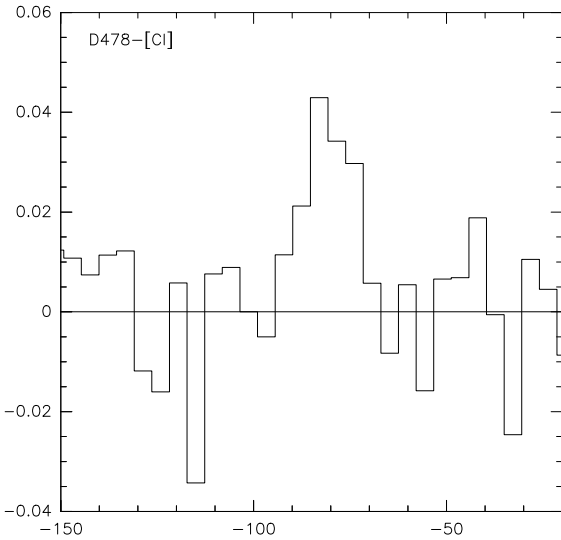


Fig. 1. [CI] spectrum observed towards D 478 in M 31. The vertical scale is $T_A^* = 0.53 T_{mb}$ in K; the horizontal scale is velocity V_{LSR} in km s^{-1} .

Table 1. [CI] and CO in D 478

Transition	T_{mb} (mK)	ΔV km s^{-1}	$\int T_{mb} dV$ K km s^{-1}	V_{hel} km s^{-1}
$^3P_1 - ^3P_0$ [CI]	85 ± 12	15 ± 2.5	1.32 ± 0.18	-85.1
$^{12}\text{CO } J=2-1^a$	310	19.5	6.44 ± 0.15	-85.2

Notes: a. Values in a $13''$ beam (J. Lequeux, private communication)

minutes (on+off) on November 29, 1996. At the observing frequency the resolution was $10.2''$ (HPBW) compared to a pointing accuracy better than $2''$ r.m.s. Weather conditions were excellent, resulting in an overall system temperature including sky of $T_{sys} = 1365$ K. For a backend, we used the DAS digital autocorrelator system in a band of 250 MHz. The resulting spectrum was binned to a velocity resolution of 4.6 km s^{-1} . At this velocity resolution, the r.m.s. noise is about 14 mK in T_A^* . We applied a linear baseline correction only and scaled the spectrum to a main-beam brightness temperature, $T_{mb} = T_A^*/\eta_{mb}$ using $\eta_{mb} = 0.53$. Line parameters were determined by gaussian fitting; the results are given in Table 1. The spectrum is shown in Fig. 1.

3. Results and analysis

and Astronomy Research Council of the United Kingdom, the Netherlands Organisation for Scientific Research, and the National Research Council of Canada.

3.1. [CI]/CO ratio

The $10''$ [CI] profile in Fig. 1 is very similar to those of $^{12}\text{CO } J=2-1$ and $J=3-2$ at $15''$ (Loinard & Allen 1998), suggesting similar spatial distributions of CO and C. The effect of resolution may be estimated by comparing the $^{12}\text{CO } J=2-1$ at a full resolution of $13''$ (kindly supplied by J. Lequeux, see Table 1) with the ^{12}CO result convolved to $23''$ given by Allen et al. (1995). In amplitude, the full resolution profile is a factor 1.35 higher and in area it is a factor of 1.18 greater. We therefore feel confident in comparing the $[\text{CI}]/^{12}\text{CO } J=2-1$ ratios resulting from our Table 1 to the CO ratios implicit in Allen et al. (1995 – their Table 1). It then follows that the [CI] 492 GHz line is similar in strength to the $^{13}\text{CO } J=1-0$ line, and considerably stronger than the $^{13}\text{CO } J=2-1$ line. Specifically, we find $[\text{CI}]/^{13}\text{CO}(2-1) = 2.0 \pm 0.5$. This is similar to the ratios 0.8 – 1.7 found at various translucent regions in the dark Galactic cloud L 183 (Stark et al. 1996), somewhat higher than the corresponding range 0.9 – 1.3 found in the Galactic dark cloud TMC-1 (Schilke et al. 1995) and rather higher than the ratio of 0.8 characterizing the Orion Bar region (Tauber et al. 1995). For this reason, we decided to also include translucent conditions, characterized by low CO and C column densities, in our analysis in addition to two-component models of the type considered by Allen et al. (1995), or the extremely low temperature model by Loinard & Allen (1998).

3.2. Model calculations

Our approach is the following. We first use radiative transfer models to explore the parameter space allowed by the observed line ratios. We then use the [CI] observations and chemical model results (van Dishoeck & Black 1988; see also van Dishoeck 1998) to further constrain the parameters thus found.

3.2.1. Radiative transfer modelling

In order to constrain the range of possible cloud parameters consistent with the observed line ratios, we have performed statistical equilibrium calculations to determine the population distribution over the ground triplet levels of [CI] and the lower ^{12}CO and ^{13}CO rotational levels, using an escape probability method for the radiative transfer (cf. Jansen 1995; Jansen et al. 1994). These calculations include collisional excitation and de-excitation as well as spontaneous and stimulated radiative transfer. The equations have been solved to find the level populations for a range of carbon and carbon monoxide column densities $N(^{12}\text{CO})$, $N(^{13}\text{CO})$ and $N(\text{C})$, kinetic temperatures T_{kin} and H_2 volume densities $n(\text{H}_2)$. We included a cosmic background radiation field of 2.75 K. and an incident radiation field $I_{UV} \approx 0.5$ (I_{UV} corresponding to $I_{1000} = 4.5 \times 10^{-8} \text{ photons s}^{-1} \text{ cm}^{-2}$).

Table 2. Model parameters and line ratios in D 478

	Single-Component Models			Two-Component Models				Observed	
T_{kin}	(K)	6	10	14	6, 6	6, 10	10/10	10/14	
Weight		—	—	—	1/2, 1	1, 1	1/6, 1	1/4, 1	
$n(\text{H}_2)$	(cm^{-3})	5000	1500	750	3000, 100				
$N(^{13}\text{CO})/\text{dV}$	($10^{14} \text{ cm}^{-2}/\text{km s}^{-1}$)	4	7	8	20, 2	20, 2	60, 6	52, 5	
$N(^{12}\text{CO})/\text{dV}$	($10^{16} \text{ cm}^{-2}/\text{km s}^{-1}$)	0.8	1.3	1.7	72, 7.2				
$N(\text{C})/\text{dV}$	($10^{16} \text{ cm}^{-2}/\text{km s}^{-1}$)	6	2.5	2	120, 160	30, 105	15, 80	5, 70	
$^{12}\text{CO} (2-1)/(1-0)$		0.46	0.46	0.46	0.40	0.46	0.45	0.48	0.42 ± 0.08^a
$^{12}\text{CO} (3-2)/(2-1)$		0.12	0.21	0.26	0.32	0.30	0.28	0.32	0.33 ± 0.10^b
$^{13}\text{CO} (2-1)/(1-0)$		0.40	0.40	0.40	0.34	0.35	0.48	0.50	0.45 ± 0.15^a
$^{12}\text{CO}/^{13}\text{CO} (1-0)$		7.4	7.8	7.8	7.4	7.4	8.5	8.7	8.8 ± 1.8^a
$^{12}\text{CO}/^{13}\text{CO} (2-1)$		8.5	8.7	9.1	8.4	9.7	7.5	8.5	8.4 ± 1.7^a
CI/ $^{12}\text{CO} (2-1)$					0.24				0.24 ± 0.05^c

Notes: a. Derived from Allen et al. (1995); b. Derived from Loinard & Allen (1998); c. This Paper.

As we have four independent CO line ratios, single-component CO models are, in principle, fully constrained by the four adjustable parameters. In practice, relatively large observational uncertainties allow only fitting of three parameters as a function of the fourth, for which we have chosen $T_{\text{kin}} = 6, 10$ and 14 K. Neutral carbon column densities are adjusted to yield, at the relevant kinetic temperature, the observed [CI]/ $^{12}\text{CO} (2-1)$ ratio of 0.24. By combining these with the model calculations of van Dishoeck & Black (1988), we then estimate the gas-phase carbon fraction $N_{\text{C}}/N_{\text{H}} = (N(\text{CO}) + N(\text{C}))/2N(\text{H}_2 + \text{N}(\text{HI}))$. From Bajaja & Shane (1982) and Brinks & Shane (1984) we find a neutral hydrogen column density $N(\text{HI}) = 1.8 \times 10^{20} \text{ cm}^{-2}$ at the position of D 478.

Parameters thus determined for single-component models are shown in Table 2, together with corresponding model line ratios. Although these models generally yield greater differences between the $^{12}\text{CO} (2-1)/(1-0)$ and $(3-2)/(2-1)$ ratios than observed, the 14 K model fits the observations within the errors. The 10 K model is barely consistent and the 6 K model fails to reproduce the observed ratios, predicting too low a $^{12}\text{CO} J = 3-2$ strength. Loinard & Allen (1998) have argued that the ^{12}CO structure of D 478 can be explained by a large, dense and very smooth cloud in LTE at even lower temperatures close to that of the cosmic background. Although it is possible to reproduce the ^{12}CO line ratios in this manner, the observed $^{13}\text{CO} (2-1)/(1-0)$ ratio of about 0.5 is only obtained at high ^{13}CO optical depths requiring $^{12}\text{CO}/^{13}\text{CO}$ ratios of order unity, which is clearly not the case. Alternatively, the observed $^{12}\text{CO}/^{13}\text{CO}$ ratios can be reproduced with lower ^{13}CO optical depths satisfying one of the two observed $^{12}\text{CO}/^{13}\text{CO}$ ratios, but the $^{13}\text{CO} (2-1)/(1-0)$ ratio then is only a third of the actually observed value.

For such reasons, Allen et al. (1995) concluded to the necessity of a model incorporating at least two components. In their analysis, they modelled the CO emission

from D 478 with two different density/temperature components, and showed that the observed line ratios are, for instance, reproduced by a cold low-density gas ($T_{\text{k}} \approx 4$ K, $n_{\text{H}} = 100 \text{ cm}^{-3}$, $\text{dV} = 5 \text{ km s}^{-1}$) and a high-density gas ($T_{\text{k}} = 7$ K, $n_{\text{H}} = 3000 \text{ cm}^{-3}$, $\text{dV} = 10 \text{ km s}^{-1}$), both with a low surface-filling factor.

We have also calculated two-component models. As there are eleven adjustable parameters (six column densities, two densities, two temperatures and the relative contributions of the two components to the total emission), no unique solution can be obtained. We have chosen to model the same H_2 densities as given in the example by Allen et al. (1995) and similar ^{12}CO column densities, and calculate the remaining parameters as a function of temperature. Furthermore, we require the column density ratio of the tenuous and the dense components to be the same for ^{13}CO and for ^{12}CO . Over the range of applicable parameters, the [CI] emission from the dense component is more efficiently produced (i.e. characterized by a higher ratio of [CI] intensity to carbon column density) than that from the tenuous component. By taking the maximum permissible contribution from the dense component, and ascribing the remainder to the tenuous component, we have minimized overall neutral carbon column densities required, and thus maximized permitted total hydrogen column densities. Although other combinations of input parameters are possible, the range of admissible parameters is nevertheless limited by the observations. For instance, changes in the assumed H_2 densities and ^{12}CO column densities, immediately require adjustment of the relative weights of the two components in order to reproduce the same line ratios which tends to minimize the effect of these changes on the parameter ratios as well.

In Table 2, we present four such cases, for temperatures varying from 6 to 14 K. As an example, the 6/6 K case corresponds closest to the example given by Allen et al. (1995), with the surface filling factor of the low-density

component twice that of the high-density component. For this case, we obtain a reasonable fit for a $^{12}\text{CO}/^{13}\text{CO}$ column-density ratio of 360. If, instead, we require the column density ratio to be 90, ^{13}CO optical depths increase significantly and we obtain for the same relative filling factors a $^{12}\text{CO}/^{13}\text{CO}$ temperature ratio of less than 4, inconsistent with the observed values. This may be repaired by increasing the relative filling factors to 1:6 or higher, but then the $^{12}\text{CO } J=2-1/J=1-0$ and especially the $J=3-2/J=2-1$ ratios drop to unacceptably low values of 0.32 and 0.19 respectively.

As Table 2 shows, increasing the temperature generally leads to higher $^{12}\text{CO}/^{13}\text{CO}$ ratios, lower ratios of neutral carbon to CO column density and a lower required contribution of the dense component. The dense component has low $N(\text{C})/N(\text{CO})$ ratios characteristic of Giant Molecular Cloud complexes in the Milky Way (0.1–0.2: Keene et al. 1985), whereas the tenuous component exhibits ratios similar to those found in Galactic translucent and dark clouds (0.3–3: Stark & van Dishoeck 1994; Stark et al. 1996).

If we increase the temperature of the dense component over that of the tenuous component, the ^{13}CO column densities change only by a small amount, the implied C column densities decrease and the relative contribution of the tenuous component also decreases. The predicted line ratios, although somewhat different, are consistent with the observed ratios. Thus, from a radiative-transfer point of view, the temperature of D 478 is not strongly constrained in a two-component model, although we note that the higher temperature (10/10 K and 10/14 K) models give slightly better fits to the observed line ratios. In the models in Table 2, the [CI] emission is optically thick at 6 K, and optically thin at 14 K. In all cases, the expected strength of the 809 GHz line is (much) less than 10 per cent of that of the 492 GHz line. As neutral carbon radiates ineffectively at temperatures below 10 K, the observed [CI] intensity rapidly requires very large C column densities and high $N(\text{C})/N(\text{CO})$ ratios if lower temperatures are assumed. This again rules out satisfactory solutions at very low temperatures.

4. Discussion

4.1. The environment of D 478

We have used the chemical models by van Dishoeck & Black (1988) assuming an incident radiation field $I_{\text{UV}} \approx 0.5$, corresponding to $I_{1000} = 2.25 \times 10^{-8}$ photons $\text{s}^{-1} \text{cm}^{-2}$. Is this a realistic value? No measurements at $\lambda = 100$ nm exist for M 31, but we may estimate the value of I_{UV} at the location D 478 by using data obtained at 155 nm (Carruthers et al. 1978; Wu et al. 1980; Israel et al. 1986). After a correction of $E(B - V) = 0.11$ for Galactic foreground extinction only, we find from these data an irradiation of D 478 by about $I_{1550} = 2.5 \times 10^{-8}$ photons

$\text{s}^{-1} \text{cm}^{-2}$. A similar result was obtained independently by Koper (1993). About 60% of this originates in the relatively nearby M 31 bulge, while about 40% is contributed by the more distant star-forming ring. A somewhat uncertain extrapolation of the 155 nm fluxes to $\lambda = 100$ nm then suggests irradiation by $I_{\text{UV}} \approx 0.3-0.4$, i.e. close to the assumed value. A substantially lower value of $I_{\text{UV}} \approx 0.1$ would change our conclusions only slightly: it would require lower H_2 column densities, and somewhat higher carbon abundances. In the absence of measurements, we have neglected the possible presence of ionized carbon (C^+). If C^+ is present in any significant amount, it would raise the total carbon column N_{C} and lower the fraction of all carbon contained in CO. In turn, this would tend to lower the resulting H_2 column densities, and lead to significantly higher carbon abundances.

The models would be better constrained if we had an independent way of estimating total hydrogen or molecular hydrogen column densities. This would be the case if, for instance, the CO intensity to H_2 column density conversion factor X or the carbon abundance in the center of M 31 were known. Unfortunately, neither is well-determined. In the disk of our Galaxy, a conversion factor of $X = 2 \times 10^{20} \text{ mol cm}^{-2} (\text{K km s}^{-1})^{-1}$ (Strong & Mattox 1996) applies, within a factor of two. However, in the central part of the Galaxy X is a factor of 3–10 lower (Sodroski et al. 1995), whereas in low-metallicity environments X may be up by one or even two orders of magnitude (Israel 1997).

Oxygen abundances in HII regions and supernova remnants in the disk of M 31, studied by Blair et al. (1982), indicate the presence of a gradient, whose extrapolation inwards yields an [O]/[H] abundance of about 1.3×10^{-3} at the galactocentric radius of D 478. Data summarized by Garnett et al. (1995) and Kobulnicky & Skillman (1998) suggest that at such high oxygen abundances, the ratio of carbon to oxygen abundances is given by $\log [\text{C}]/[\text{O}] = -0.2 \pm 0.3$ so that $[\text{C}]/[\text{H}] = 8(+8, -4) \times 10^{-4}$. This result has a large uncertainty, however, because no direct abundance measurements exist within $R = 5$ kpc, because the M 31 disk data exhibit a relatively large scatter, and because the relation between [O]/[H] and [C]/[O] abundances is not well-established at such high [O]/[H] abundances. In addition, a significant fraction of all carbon in quiescent dark clouds such as D 478 is expected to be depleted onto dust grains, leaving actual gas-phase carbon abundances substantially lower, by factors of order $\delta_{\text{C}} \approx 0.4$. This would lead us to expect total column density ratios $N_{\text{C}}/N_{\text{H}} \approx 3 \times 10^{-4}$.

Moreover, an inward extrapolation from the disk may not be representative of conditions in D 478. The velocity of D 478 is anomalously low for its projected distance to the nucleus. In position-velocity maps presented by Brinks & Shane (1984), one of which is reproduced by Loinard et al. (1995), it coincides with a loop-like HI structure. This structure exhibits a north-south symmetry with respect

Table 3. Beam-averaged parameters for D 478

	Units	Single-Component Models			Two-Component Models			
T_{kin}	(K)	6	10	14	6, 6	6, 10	10, 10	10, 14
$N(^{12}\text{CO})$	(10^{16} cm^{-2})	5	4	4	160	135	50	45
$N(\text{C})$	(10^{16} cm^{-2})	26	6	4	130	35	25	15
$N(\text{C})/N(\text{CO})$		5	1.5	1	0.8	0.3	0.5	0.3
N_{C}	(10^{16} cm^{-2})	31	10	8	290	170	75	60
N_{H}	(10^{21} cm^{-2})	1.6	1.7	1.2	3.5	4	2	2
$N_{\text{C}}/N_{\text{H}}$	(10^{-4})	2	0.6	0.7	8	4.5	3.5	3
$N(\text{H}_2)$	(10^{21} cm^{-2})	0.7	0.7	0.5	1.7	1.8	1.0	0.9
$f(\text{H}_2)$ (dense)		0.22	0.11	0.10	0.27	0.27	0.06	0.06
$f(\text{H}_2)$ (tenuous)		—	—	—	0.54	0.27	0.33	0.24
$N(^{12}\text{CO})/N(\text{H}_2)$	(10^{-4})	0.7	0.5	0.8	9.5	7.5	5	5
dM/dA	($M_{\odot} \text{ pc}^{-2}$)	4	4	3	9	9	5	5
X	($10^{20} \text{ cm}^{-2} (\text{K km s}^{-1})^{-1}$)	0.5	0.5	0.3	1.1	1.2	0.7	0.6

to the center, but is most pronounced north of the center. It appears to represent rapidly rotating gas in the inner part of M 31, moving in inclined elliptical orbits in a weak bar-like potential (cf. Stark & Binney 1994). D 478 is located close to the northern tangential point of this rotating structure. It is conceivable that this is the signature of a merging event in which a small late-type galaxy fell into the large spiral M 31. Such a notion is supported by the presence of a double nucleus in M 31 (cf. Lauer et al. 1993). In that case, the metallicity of the inner gas clouds may be substantially lower than expected from extrapolation of the disk gradient. If the metallicity is comparable to that of the outer disk of M 31 we have $[\text{O}]/[\text{H}] = 4 \times 10^{-4}$ and again following Garnett et al. (1995) we find a low total carbon abundance $[\text{C}]/[\text{H}] = 1.5 \times 10^{-4}$. Taking into account depletion, this case would lead us to expect $N_{\text{C}}/N_{\text{H}} \approx 0.7 \times 10^{-4}$.

4.2. Conditions in D 478

In Table 3, we have used the ratio of the observed to model line intensities to calculate *beam-averaged* column densities of carbon monoxide and neutral carbon, as well as those of total carbon (C + CO), total hydrogen, and molecular hydrogen. We have used the total hydrogen column densities, multiplied by 1.35 to take into account a contribution by helium, to calculate the projected mass density dM/dA (corrected by $\cos i$ with $i = 77^\circ$) and we also determined the CO – H₂ conversion factor X . As shown in the preceding section, we have, if anything, overestimated hydrogen column densities (and masses), and underestimated carbon abundances. In addition, we have estimated surface filling factors $f(\text{H}_2)$ by dividing the observed velocity-integrated line intensities by the model intensities, and assuming that the surfaces covered by CO and by H₂ are identical.

First we consider the single-density models. The physical equivalent of these models is that of high-density filamentary clouds rather uniformly but incompletely filling a large surface area. We have already ruled out the model for $T_{\text{k}} = 6$ K, because it does not reproduce the observed $^{12}\text{CO } J=3-2$ intensity. Both the 10 K and 14 K models fit the observed intensities although the predicted $^{12}\text{CO } J=3-2$ intensity is low compared to the observed value (Table 2), rendering the 10 K model in particular somewhat marginal. However, single-component models are consistent only with *low* $[\text{C}]/[\text{H}]$ ratios. They are ruled out if we accept the extrapolated high carbon abundances, but would be just consistent with an anomalously low metallicity as discussed above. The single-density models furthermore require rather low $^{12}\text{CO}/^{13}\text{CO}$ abundance ratios of about 20. This is not out of the question, because in cold diffuse and translucent clouds, such as described by the single-density models in Table 2, ion-molecule exchange reactions may favour the formation of ^{13}CO at the expense of ^{12}CO for temperatures $T_{\text{k}} < 36\text{K}$ although ^{13}CO remains more susceptible to photodissociation than ^{12}CO . Surface filling factors are between 0.2 and 0.1, the lower values pertaining to the higher temperatures. The relatively low H₂ column densities imply projected mass densities of only about $4 M_{\odot} \text{ pc}^{-2}$ (Table 3), and X values about five times lower than those in the Solar Neighbourhood. We conclude that for D 478 single-component models at temperatures $T_{\text{kin}} \geq 10$ K on the one hand cannot be ruled out, but on the other hand do not appear to be very convincing.

The two-density models provide better fits to the observations; like the single-component models they have average H₂ column densities below the star formation threshold in keeping with the quiescent appearance of D 478. The 6/6 K model requires a relatively large $N_{\text{C}}/N_{\text{H}}$ ratio of eight, implying a total carbon abundance $[\text{C}]/[\text{H}] \geq 2 \times 10^{-3}$ which seems rather high. More reasonable

carbon abundances would imply higher H_2 column densities and projected gas mass densities, but the large neutral carbon column densities required by the observed line strength at the assumed temperature of 6 K would then imply $N(\text{C})/N(\text{CO})$ ratios much larger than allowed at such column densities.

With increasing temperature, the CO and [CI] column densities required by the observed line emission become more modest. Because the carbon/hydrogen column density ratio also drops, total hydrogen and molecular hydrogen column densities change relatively little. At these temperatures, $N_{\text{C}}/N_{\text{H}} \approx 4 \times 10^{-4}$, which corresponds to a total carbon abundance $[\text{C}]/[\text{H}] \approx 1 \times 10^{-3}$ if $\delta_{\text{C}} = 0.4$. This is about 2.5 times the value ascribed to the Solar Neighbourhood, and close to the value expected from the extrapolation of M 31 disk abundances. The CO intensity to H_2 column density value for these models is relatively well-determined with $X = 0.9 \pm 0.3 \times 10^{20} \text{ mol cm}^{-2} (\text{K km s}^{-1})^{-1}$, or about half of the Solar Neighbourhood value. Projected mass densities are in the range of 5–9 $M_{\odot} \text{ pc}^{-2}$. Surface filling factors for the emission within the beam are given in Table 3 for both the high-density and the low-density components; the ratio of the two is for each model, of course, equal to the ratio of the weights given in Table 2. Again, the lower temperature models have the largest filling factors. The two models with dense gas temperatures of 10 K yield surface filling factors of 6% for the dense gas and about 30% for the tenuous gas. These values appear to be consistent with the small fraction (15%) of the single-dish CO flux recovered in the interferometric map by Loinard & Allen (1998). The model H_2 column densities divided by the input H_2 densities provides a measure for the line-of-sight depth z through the clouds in the emitting surface fraction. For the two-component models in Table 3, we find $0.3 \text{ pc} \leq z_d \leq 0.7 \text{ pc}$ and $4.5 \text{ pc} \leq z_t \leq 7.5 \text{ pc}$. The subscripts d and t refer to the dense and the tenuous components respectively, and the larger depths occur at the higher temperatures. Both the surface filling factors and the subcloud depths suggest that the structure of D 478 is highly fragmented and filamentary.

The models discussed do not fully constrain the physical conditions applying to D 478. Various other combinations of parameters could be used as input. Multi-density models incorporating temperature gradients might be better representations of the actual structure of D 478, and could easily be made to satisfy the observations. For instance, adding a contribution of material at intermediate densities and temperatures to the two-component models in Table 2 within the limits imposed by observed line ratios would indeed change the detailed set of physical parameters, but would not substantially change the overall result. We conclude that the observations of D 478, and in particular the relatively strong [CI] emission appear to rule out the presence of very large amounts of molecular gas at very low temperatures in this complex. At the very least, our models show that there is no compelling need to

assume such a state of affairs. The interferometric results obtained by Loinard & Allen (1998) indicate a relatively small contribution by dense, compact material. This suggests that the 10/10 K and 10/14 K models with their small surface-filling fraction of the dense component are a better representation than the lower-temperature models.

Most likely, D 478 is rather similar to dark cloud complexes in our own Galaxy, at the higher metallicity consistent with its central location in M 31. It has a modest projected mass density and a relatively low X -factor, both of which are consistent with this conclusion. A comparison with the Galactic Taurus-Auriga dark cloud complex at a distance of 140 pc is illustrative. We have already noted similar $[\text{CI}]/^{13}\text{CO}$ (2-1) ratios (Schilke et al. 1995). Likewise, the Taurus ^{12}CO (2-1)/(1-0) ratio of 0.53 (Sakamoto et al. 1997) is close to that of D 478. More in detail, an area 30° (80 pc) across was mapped in CO by Ungerechts & Thaddeus (1987). Ignoring the more distant and unrelated clouds, we find that the mean integrated line intensity of the complex is 4.5 K km s^{-1} with individual clouds having intensities between 3 and 15 K km s^{-1} . The surface filling factor of the complex is 0.3, and its appearance is indeed very fragmented and clumpy. The complex has a mean mass-density $dM/dA = 7 M_{\odot} \text{ pc}^{-2}$. Both the observed line ratios and the derived quantities thus suggest that D 478 is similar to a larger version of the Taurus-Auriga dark cloud complex.

Assuming an overall cloud size of $1'$ (Allen & Lequeux 1993) and including a contribution by helium, the gas mass of D 478 is of the order of $1 \times 10^6 M_{\odot}$. This is an order of magnitude lower than the virial mass deduced by Allen & Lequeux (1993) and Loinard & Allen (1998). However, it is doubtful whether molecular cloud complexes are virialized at all. Moreover, the shape of the line profiles of D 478 suggests the presence of at least two distinct components. Its location near the tangential point of a rapidly rotating structure with noncircular motions suggests that various individual clouds, separated by significant distances, may be seen with very similar velocities in the same line of sight; the appearance of the HI distribution in the position-velocity maps published by Brinks & Shane (1984) lends credibility to this suggestion. In this respect it is relevant to note that the velocity width of line spectra incorporating emission of various unrelated clouds in the same beam will reflect the cloud-cloud velocity dispersion of about 9 km s^{-1} (Stark 1979) in addition to any systematic velocity shifts and the velocity widths of the individual clouds. Applying the virial equation to such a collection of clouds will lead to a potentially large overestimate of the actual mass.

5. Conclusions

1. We have detected the 492 GHz emission line from the $^3\text{P}_1 - ^3\text{P}_0$ [CI] transition towards the dark cloud D 478 in M 31. The [CI] line strength is comparable to that of

- $^{13}\text{CO } J=1-0$ and about twice as strong as that of the $^{13}\text{CO } J=2-1$ transition. This is similar to the intensity ratios found in Galactic dark and translucent clouds.
- We have used ^{12}CO and ^{13}CO intensities from the literature together with the newly determined [CI] intensity to model conditions in the D 478 cloud complex. We have considered both single-density filamentary clouds and two-density core/envelope clouds. In particular, inhomogeneous (two-component) models produce good fits to the observations. Dense core $N(\text{C})/N(\text{CO})$ ratios are found to be similar to those of Giant Molecular Clouds in the Milky Way, whereas the ratios derived for the extended more tenuous gas are similar to those found in Galactic dark and translucent clouds.
 - D 478 appears to be similar to Galactic dark cloud complexes, such as the Taurus-Auriga dark cloud complex. Most likely, it is characterized by a higher metallicity consistent with an extrapolation of M 31 disk abundances to its central location in the galaxy. Its kinetic temperature is of the order of 10 K. There appears to be no need to assign very low temperatures and very high H_2 mass densities to the D 478 complex; our results do not support the virial mass surface densities of D 478 of $\sim 100 M_{\odot} \text{pc}^{-2}$ suggested by Loinard & Allen (1998).
 - Actual cloud mass densities projected onto the M 31 midplane are of the order of $5-10 M_{\odot} \text{pc}^{-2}$. The CO to H_2 conversion factor is $X = 0.9 \pm 0.3 \times 10^{20} \text{cm}^{-2} (\text{K km s}^{-1})^{-1}$, about half the value in the Solar Neighbourhood.
 - The D 478 complex may not be a single entity, but instead may consist of various clouds at different locations projected onto the same line-of-sight towards the tangential direction of a rapidly rotating structure characterized by noncircular velocities.

Acknowledgements. We are indebted to Ewine van Dishoeck and David Jansen from the Leiden astrochemistry group for letting us use their statistical equilibrium calculation models and benefitted from discussions with Ewine van Dishoeck. We also thank James Lequeux for kindly providing us with the unpublished full-resolution parameters of the $^{12}\text{CO } J=2-1$ profile of D 478. Critical remarks on an earlier draft by Ron Allen and Lasurent Loinard led to a substantial improvement in the paper.

References

Allen R.J., Lequeux J., 1993 ApJL 410, L15
 Allen R.J., Le Bourlot J., Lequeux J., Pineau des Forêts G., Roueff E., 1995 ApJ 444, 157
 Bajaja E., Shane W.W., 1982 A&AS 49, 745
 Berkhuijsen E.M., Bajaja E., Beck R., 1993 A&A 279, 359
 Blair W.P., Kirshner R.P., Chevalier R.A., 1982 ApJ 254, 50
 Blitz L., 1985 ApJ 296, 481
 Brinks E., Shane W.W., 1984 A&AS 55, 179
 Carruthers G.R., Heckathorn H.M., Opal C.B., 1978 ApJ 225, 346

Casoli F., Combes F., 1988 A&A 198, 43
 Casoli F., Combes F., Stark A.A., 1987 A&A 173, 43
 Garnett D.R., Skillman E.D., Dufour R.J., et al. 1995 ApJ 443, 64
 Hodge P.W., 1980 AJ 85, 376
 Israel F.P., 1997 A&A 328, 471
 Israel F.P., de Boer K.S., Bosma A., 1986 A&AS 66, 117
 Jansen D.J., 1995 Ph.D. thesis, University of Leiden (NL)
 Jansen D.J., van Dishoeck E.F., Black J.H., 1994 A&A , 282, 605
 Keene J., Blake G.A., Phillips T.G., Huggins P.J., Beichman C.A., 1985 ApJ 299, 967
 Kobulnicky H.A., Skillman E.D., 1998 ApJ 497, 601
 Koper E., 1993 Ph.D. Thesis Leiden University (NL)
 Kutner M.L., Verter F., Rickard L.J., 1990 ApJ 365, 195
 Lada C.J., Margulis M., Sofue Y., Nakai N., Handa T., 1988 ApJ 328, 143
 Lauer, T.R., Faber S.M., Groth E.J., et al. 1993 AJ 106, 1436
 Loinard L., Allen R.J., 1998 ApJL 499, 277
 Loinard L., Allen R.J., Lequeux J., 1995 A&A 301, 68
 Loinard L., Allen R.J., Lequeux J., 1996a A&A 310, 93
 Loinard L., Dame T.M., Koper E., Lequeux J., Thaddeus P., Young J.S., 1996b ApJL 469, L101
 Nakano M., Ichikawa T., Tanaka Y.D., Nakai N., Sofyu Y., 1987 PASJ 39, 57
 Ryden B.S., Stark A.A., 1986 ApJ 305, 823
 Sakamoto S., Hasegawa T., Handa T., Hayashi M., Oka T., 1997 ApJ 486, 276
 Sandqvist Aa., Elfhag T., Lindblad P.O., 1989 A&A 218, 39
 Schilke P., Keene J., Le Bourlot J., Pineau des Forêts G., Roueff E., 1995 A&A 294, L17
 Sodroski T.J., Odegard N., Dwek E., et al. 1995 ApJ 452, 262
 Stark A.A., 1979 Ph.D Thesis Princeton Univ. (USA)
 Stark A.A., Binney J., 1994 ApJL 426, L31
 Stark R., van Dishoeck E.F., 1994 286, L43
 Stark R., Wesselius P.R., van Dishoeck E.F., Laureijs R.J., 1996 A&A 311, 282
 Strong A.W., Mattox J.R., 1996 A&A 308, L21
 Tauber J.A., Lis D.C., Keene J., Schilke P., Büttgenbach T.H., 1995 A&A 297, 567
 Ungerechts H., Thaddeus P., 1987 ApJS 63, 645
 van Dishoeck E.F., 1998, in: *The Molecular Astrophysics of Stars and Galaxies – A Volume Honouring Alex Dalgarno*, eds. T.W. Hartquist & D.A. Williams, Oxford University Press, in press
 van Dishoeck E.F., Black J.H., 1988 ApJ 334, 771
 Vogel S.N., Boulanger F., Ball R., 1987 ApJL 321, L145
 Wilson C.D., Rudolph A.R., 1993 ApJ 406, 477
 Wu, C.-C., Faber S.M., Gallagher J.S., Peck M., Tinsley B.M., 1980 ApJ 237, 290